C Journal of Carbon Research

MDPI

Communication

Is the Formation of Poly-CO_2 Stabilized by Lewis Base Moieties in N- and S-Doped Porous Carbon?

Saunab Ghosh [1] and Andrew R. Barron [1,2,3,*]

[1] Department of Chemistry, Rice University, Houston, TX 77005, USA; sg4668@rice.edu
[2] Department of Materials Science and Nanoengineering, Rice University, Houston, TX 77005, USA
[3] Energy Safety Research Institute, Swansea University Bay Campus, Swansea SA2 8QQ, UK
* Correspondence: arb@rice.edu; Tel.: +1-713-348-5610

Academic Editor: Enrico Andreoli
Received: 8 January 2016; Accepted: 5 February 2016; Published: 15 February 2016

Abstract: The polymerization of CO_2 by Lewis basic moieties has been recently proposed to account for the high adsorption ability of N and S-doped porous carbon materials formed from the pyrolysis of sulfur or nitrogen containing polymers in the presence of KOH. *Ab initio* calculations performed on the ideal CO_2 tetramer complex LB-$(CO_2)_4$ (LB = NH_3, H_2O, H_2S) showed no propensity for stabilization. A weak association is observed using Lewis acid species bound to oxygen (LA = H^+, AlF_3, AlH_3, B_4O_6); however, the combination of a Lewis acid and base does allow for the formation of polymerized CO_2 (*i.e.*, LB-C(O)O-$[C(O)O]_n$-C(O)O-LA). While the presence of acid moieties in porous carbon is well known, and borate species are experimentally observed in KOH activated porous carbon materials, the low stability of the oligomers calculated herein, is insufficient to explain the reported poly-CO_2.

Keywords: porous carbon; nitrogen; sulfur; poly-CO_2; *ab initio*; Lewis acid; Lewis base

1. Introduction

It has recently been reported by Hwang *et al.* [1] that pyrolysis of sulfur or nitrogen containing polymers in the presence of KOH results in a highly porous carbon materials, which were shown to exhibit a relatively high uptake of CO_2 (0.82 g CO_2/g sorbent @ 30 bar). Nitrogen-containing porous carbon (NPC) materials have previously been reported to be active for CO_2 capture. In general, their uptake was in the range of 0.14–0.19 g CO_2/g sorbent @ 1 bar [2–5]. Analysis of the reported data by Hwang *et al.*, shows an uptake of between 0.11–0.19 g CO_2/g sorbent @ 1 bar [1], *i.e.*, within the range exhibited for prior materials. The high surface area/high porosity was proposed to be as a consequence of reactivity with KOH prior to pyrolysis. However, this approach is well known in the literature, for example, a similar method has been reported by Chandra, *et al.* [5] and investigated in detail [6], while the same N-containing polymers were reported to be porous carbon precursors that could be activated by KOH by Sevilla *et al.* [3]. Furthermore, sulfur containing porous carbon (SPC) has also been reported by Sevilla *et al.* [7] using the identical route to that subsequently reported by Hwang *et al.* [1]; the only difference was the measurement at high pressures in the latter study.

The suggested adsorption at high pressure was proposed [1] to be due to the polymerization of the CO_2 to form poly-CO_2 in which the N- or S-dopant acted as a Lewis base for the initiation of polymerization, see Figure 1. Spectroscopic data was presented as evidence for the formation of poly-CO_2. In the case of Raman spectroscopy, the presence of a band at 798 cm^{-1} was similar to known spectroscopic characterization [8], while, the proposal of an ^{13}C NMR peak at δ = 166.5 ppm and IR band at 1730 cm^{-1} due to poly-CO_2 were based upon comparison with organometallic compounds of C_2O_4 [9,10]. The rationalization for the, heretofore, unknown formation of poly-CO_2 in a porous carbon matrix was by suggesting that the nitrogen (or sulfur) Lewis base species were responsible for initiating

polymerization. However, as noted above, N-doped porous carbon materials are both well-known and shown (under comparable conditions) to be efficient absorbers of CO_2 [2–5]. Furthermore, except at high pressures and temperatures (40 GPa, 1800 K [8]) the only examples of oligomerized CO_2 require both Lewis acid as well as Lewis base moieties [9,10]. It seems that the explanation provided is incomplete since this would have been observed previously, especially since studies at equally high pressures have been reported for a wide range of porous carbon materials [11–14].

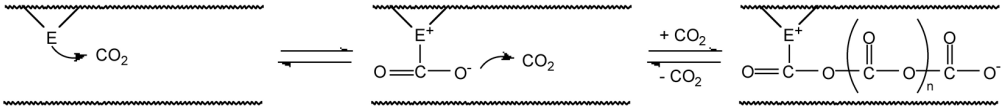

Figure 1. Proposed polymerization mechanism for the Lewis base initiated formation of poly-CO_2, where E = N or S [1].

Given that both N- and S-doped porous carbon materials have been known for some time, and their chemistry well characterized, it is curious that the formation of poly-CO_2 has not been previously reported. The report raises the question as to what is the nature of the activation of CO_2 to polymerization? Can N- or S-donor atoms alone be responsible for CO_2 polymerization? An understanding of this process would allow for the synthesis of other porous adsorbents for CO_2, in particular those with a greater selectivity as compared CH_4, N_2 *etc.* We have therefore, investigated the stabilization of poly-CO_2 with various Lewis base and Lewis acid species using *ab initio* methods.

2. Results and Discussion

Initial studies used an ideal CO_2 tetramer complex with a suitable Lewis base model (Figure 2a, LB = NH_3, H_2S, H_2O). The choice of NH_3 and H_2S was intended as a simplified model for the N- and S-dopant within the porous carbon [1]. The addition of H_2O to the study was because all the NPC and SPC materials reported also contain significant oxygen [1–5].

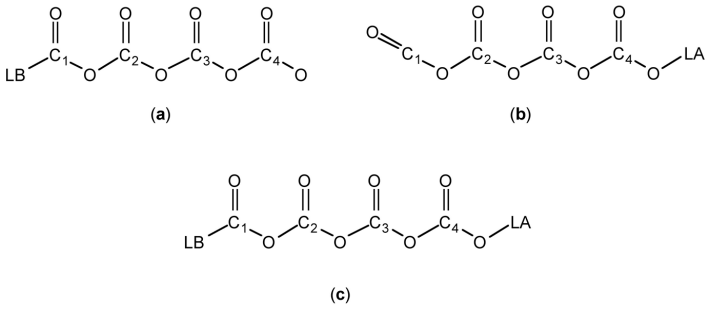

Figure 2. Ideal CO_2 tetramer complexes used as the starting point for *ab initio* calculations with (**a**) Lewis base terminus (LB = NH_3, H_2S, H_2O); (**b**) Lewis acid terminus (LA = AlF_3, B_4O_6, H^+); and (**c**) both Lewis acid and base termini. The numbers for the CO_2 carbon atoms represent the position with respect to the Lewis base end. The *syn* conformation is shown for simplicity.

Structural optimization, through energy minimization, resulted, in each case, in the complete dissociation of at least three of the CO_2 molecules. In the case of NH_3 and H_2O the remaining CO_2 is weakly associated as seen in Figure 3a,b, respectively. The N $\cdots$ C (2.561 Å) and O $\cdots$ C (2.373 Å) distances are outside of ordinary covalent interactions (1.47 and 1.43 Å, respectively), but within the sum of the van der Waals radii (3.25 and 3.22 Å, respectively) [15]. In order to determine local minima a series of starting models were used. Thus, if an all *anti* starting configuration is used as an initial model then a slightly different spatial arrangement of the uncoordinated CO_2 molecules results in an alternative local minimum, but the Lewis base $\cdots$ CO_2 interaction remains essentially constant. For the weaker Lewis base (H_2S), complete dissociation results are irrespective of starting geometry.

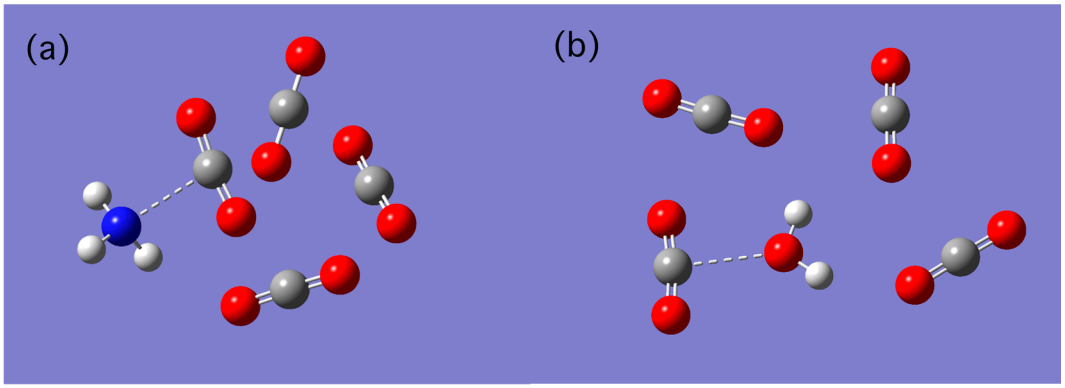

Figure 3. Optimized local minima structures for (**a**) NH_3 and (**b**) H_2O interactions with CO_2.

A convenient measure of the weak interactions is the O–C–O bond angle as a function of each CO_2's distance from the Lewis base. As may be seen from Table 1 the effects of NH_3 and H_2O are similar and limited to the first two CO_2 molecules, while that of H_2S is negligible. The dipole-dipole or van der Waal interaction is slightly exothermic; however, any attempt to move the CO_2 molecules closer results in a destabilization.

Table 1. *Ab initio* calculated geometry of the CO_2 molecules as measured by the O-C-O angle (°) for various Lewis base (LB) and Lewis acid (LA) systems [a].

LB	1	2	3	4	LA
NH_3	170.9	177.7	177.2	177.2	-
H_2S	179.9	179.8	179.9	179.0	-
H_2O	171.7	176.4	178.4	178.4	-
-	177.1	176.8	175.9	173.9	AlF_3 [b]
-	177.3 [c]	178.9	179.5	174.7	B_4O_6
-	179.6	179.4	178.1 [d]	144.3	H^+
NH_3 [e]	129.8	131.2	128.2	131.7	AlF_3
NMe_3	128.5	128.9	125.6	129.8	B_4O_6
NH_3	134.4	131.9	130.9	129.9	H^+
H_2S	135.4	132.2	131.0	129.9	H^+
H_2O	141.1	133.8	131.7	130.3	H^+

[a] The numbers represent the position of the CO_2 molecule within the starting structure, see Figure 2; [b] Local minima involving a single $CO_2 \cdots AlF_3$ interaction; [c] Also exhibits an $O \cdots B$ interaction; [d] Involved in secondary interaction with H^+; [e] Involves $N–H \cdots F$ intra-oligomer H-bond.

It would thus appear that the view provided by Hwang *et al.* [1] is insufficient to explain the presence of the spectroscopically characterized poly-CO_2. Given the isolation of oligomerized CO_2 in the presence of both Lewis acid and base moieties [9,10], we have investigated their effect on nitrogen and sulfur stabilized poly-CO_2 of a Lewis acid. In order to remove excess KOH from the reaction, the samples were reported to be washed with acid [1]. Thus, the simplest Lewis acid will be acid residue, which is simplified as H^+.

It has been found that samples prepared according to the reported procedure [1] contain variable amounts of boron (1.8%–3.5%) as determined from X-ray photoelectron spectroscopy (Figure 4). Given that the activation of the carbon precursor was with KOH and uses glassware [1] this is not unexpected. The high resolution B 1s spectrum (Figure 4b) showed a peak (193.63 eV) consistent with the B 1s peak position for sodium borate glasses (192.45 eV) [16]. As such, we have modeled potential boron Lewis acid species using the B_4O_6 cluster. Finally, AlF_3 was used as a strong Lewis acid for comparison with H^+ and B_4O_6.

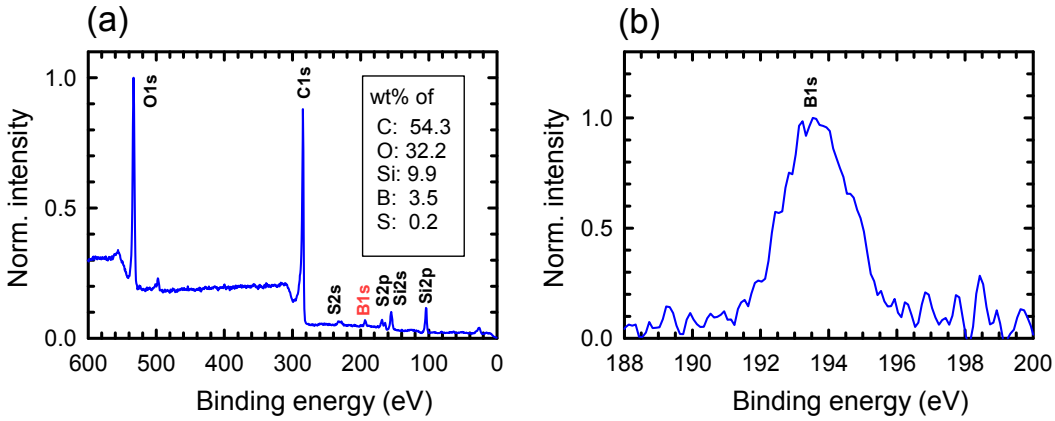

Figure 4. X-ray photoelectron spectroscopy (XPS) survey spectrum (**a**) and high resolution B 1s spectra (**b**) showing the presence of B–O species.

Initially, structural optimization was undertaken for the LA stabilized CO_2 tetramer (Figure 2b). As may be seen from Table 1, the strong Lewis acid AlF_3 shows two potential structures. The first higher energy form (Figure 5a) is of the same manner to the Lewis base derivatives (see Figure 3). The Al $\cdots$ O distance (1.881 Å) is within the range for typical Lewis acid-base interactions observed from X-ray crystallography (1.8–2.0 Å) [17–19]; however, there appears little effect on subsequent CO_2 molecules. The strong Lewis acid nature of AlF_3 and the Lewis basic nature of the fluorine ligands results in a more stable (27 kJ/mol) structure involving two CO_2 molecules occupying the axial positions of a trigonal bipyramidal aluminum; again the Al $\cdots$ O distances (2.028, 2.049 Å) are within the range for such coordination geometries about aluminum (1.890(6)–2.283(2) Å) [20]. The additional CO_2 molecules appear to show interactions with the fluorine ligands via Al–F $\cdots$ C interactions (2.44, 2.49 Å); however, again there is no poly-CO_2 stabilization. Like AlF_3, borate (B_4O_6) shows a significant primary effect (Table 1, Figure 5b) with B $\cdots$ O distances (1.594 and 1.646 Å) is slightly longer than typical Lewis acid-base interactions observed from X-ray crystallography (1.451(3)–1.502(4) Å) [21,22]. In contrast, H^+ shows a significant structural effect on both the 1st and 2nd CO_2, with diminishing results with distance (Table 1, Figure 5c). Again, as with AlF_3 the more stable form involves the H^+ hydrogen bonding between two CO_2 molecules, with the O $\cdots$ O distance (2.410 Å) being typical of an O–H $\cdots$ O hydrogen bond [23,24].

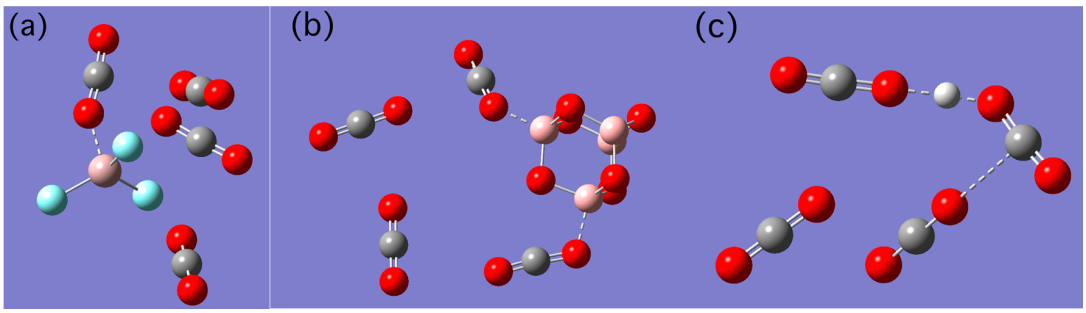

Figure 5. Optimized local minima structures for (**a**) AlF_3; (**b**) B_4O_6; and (**c**) H^+ interactions with CO_2.

From the proceeding it is clear that Lewis acid species have a similar effect on the stabilization of oligomeric CO_2 that is observed with Lewis bases. As prior structural characterization of oligomeric CO_2 involved both Lewis acid and Lewis base moieties [9,10], we have investigated the stability of LB–$(CO_2)_4$–LA, where LB = NH_3, NMe_3, H_2O, and H_2S, while LA = AlF_3, B_4O_6, and H^+ (Figure 2c). Based upon the distortion of the CO_2 molecules from linear (Table 1) and the C $\cdots$ O distances (Table 2) the combination of both Lewis acid and Lewis base has a profound effect on the geometrical changes

of each CO_2, and hence the stability of the oligomer. Energy minima are calculated starting with both the all-*syn* (c.f., Figure 2c) and all-*anti* initial structures. As such the *anti* isomer is found to be more stable than the *syn*. The data shown in Tables 1 and 2 is, therefore, for the *anti* isomer, except for H_3N–$(CO_2)_4$–B_4O_6 which upon starting with the *anti* isomer undergoes a proton transfer from ammonia to oxygen resulting in opening of the borate cage. To obviate this effect, NMe_3 was used as an "inert" analog. It is interesting to note that the "*anti*" conformer is actually a spiral structure, while the *syn* retains its planar confirmation. Representative structures are shown in Figure 6.

Table 2. *Ab initio* calculated geometry of the CO_2 molecules as measured by the intermolecular distances (Å) for various Lewis base (LB) and Lewis acid (LA) systems. [a]

LB	LB ··· C_1	O_1 ··· C_2	O_2 ··· C_3	O_3 ··· C_4	O_4 ··· LA	LA
NH_3	1.467	1.404	1.409	1.435	1.744	AlF_3
NMe_3	1.479	1.385	1.404	1.385	1.466	B_4O_6
NH_3	1.523	1.417	1.401	1.394	0.969	H^+
H_2S	1.876	1.423	1.402	1.394	0.969	H^+
H_2O	1.517	1.439	1.411	1.398	0.969	H^+

[a] The numbers represent the position of the CO_2 molecule within the starting structure, see Figure 2.

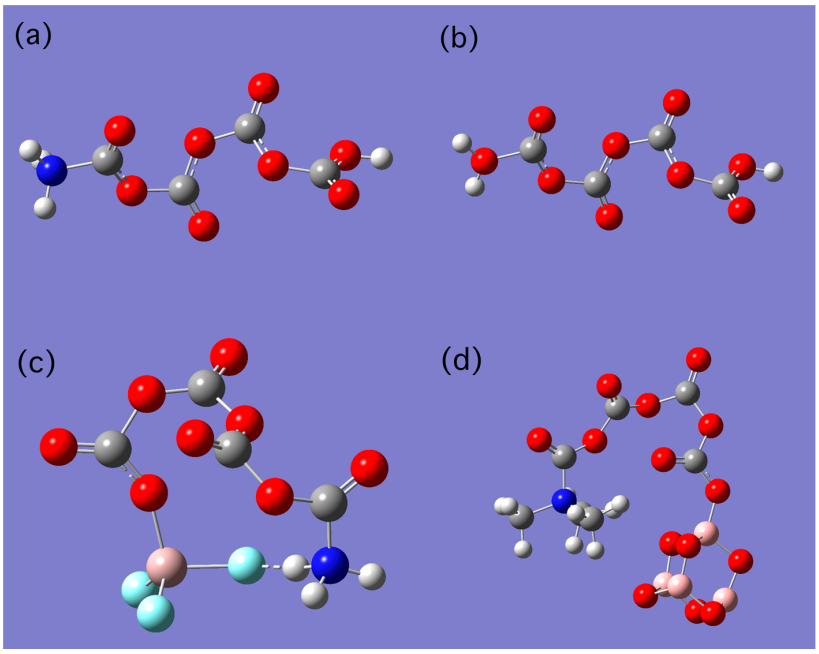

Figure 6. Optimized energy minima structures for (**a**) H_3N-$(CO_2)_4$-H^+; (**b**) H_2O-$(CO_2)_4$-H^+; (**c**) Me_3N-$(CO_2)_4$-B_4O_6; and (**d**) H_3N-$(CO_2)_4$-AlF_3.

Not all of the structures provided a simple oligomerization of the CO_2. It was found that local minimum for AlF_3 and B_4O_6 complexes sometimes involved secondary interactions. For example, in the cases of H_3N–$(CO_2)_4$–B_4O_6 proton extraction (from the Lewis base) by the strongly Lewis basic oxo-sites resulted irrespective of the initial conformation employed. Thus, Me_3N–$(CO_2)_4$–B_4O_6 was used as a model (Figure 6b). Not as marked was the secondary N–H ··· F intra-oligomer interaction observed for H_3N–$(CO_2)_4$–AlF_3 (Figure 6c).

It is worth noting that the C ··· O distances (Table 2) in the chain range between 1.385–1.439 Å, which is to the shorter side of that expected for a typical C–O single bond (1.43 Å). As may be seen, the relative effect of the Lewis acid terminus on the C ··· O distances (Table 2) is $AlF_3 > H^+ \approx B_4O_6$, while that of the Lewis base is $NH_3 \approx H_2O > H_2S$. In contrast, the O–C–O angle changes (Table 1) follow the orders $H^+ \approx B_4O_6 > AlF_3$ for the Lewis acid and $NH_3 \approx H_2S > H_2O$ for the Lewis base.

Based upon these results, it is clear that if poly-CO_2 were formed within a N- or S-doped porous carbon material then the presence of a Lewis acid would be necessary. It should be noted that in the original report [1], HCl was used to remove excess KOH from the porous carbon after pyrolysis. Although extensive washing with H_2O is described there is a possibility that residual acid was retained prior to CO_2 adsorption measurements that provided the Lewis acid species. However, experimentation with different washing protocols does not alter the CO_2 uptake of the NPC or SPC. As noted above, the use of KOH as an activator in glassware results in borate species being present. We have, therefore, investigated the activation of NPC samples using sodium metaborate tetrahydrate ($NaBO_2 \cdot 4H_2O$) and borax ($Na_2B_4O_7$), see Experimental. As may be seen from Figure 7, the CO_2 uptake for these borate activated NPC materials is significantly lower than that for KOH activated analog. Thus, the presence of borate species is not associated with high CO_2 adsorption in NPC; however, clearly KOH activation is important [3,5–7].

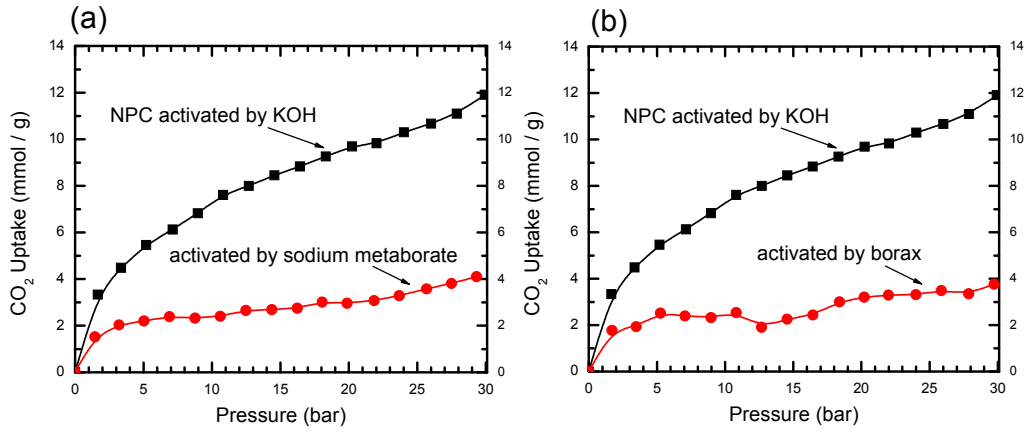

Figure 7. Plot of CO_2 uptake (mmol CO_2/g NPC) as a function of CO_2 pressure (Bar) for NPC activated with (**a**) sodium metaborate tetrahydrate and (**b**) borax as compared to NPC activated with KOH.

The presence of Lewis acid sites in porous carbons has been well characterized [25–27]. While we acknowledge that Lewis acid sites could be associated with the N content, they are ordinarily associated with oxygen moieties, such as OH groups, in porous carbon materials. Thus, it would be reasonable to propose that if poly-CO_2 species are formed at high pressure within NPC or SPC it would be stabilized by the presence of oxygen based Lewis acid sites. Attempts to model such an interaction using phenol (C_6H_5OH) as the protic source was unsuccessful; however, interaction of a Lewis acid/base model compound derived from dibenzo[a,j]anthracene (Figure 8) with excess CO_2 resulted in the formation of the trimeric CO_2 species shown in Figure 9 as a energy minimum. While only a simplified approximation of structures that could be present within NPC, this suggests that the presence of O in porous carbon materials (see Figure 4) could provide Lewis acid sites that in concert with O, N or S Lewis base species could explain the formation of poly-CO_2. However, the weakness of the $CO_2 \cdots CO_2$ interaction still posits against significant poly-CO_2 under the conditions of 25 °C and 30 Bar.

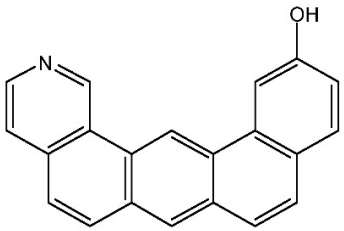

Figure 8. Structure of the bi-functional model Lewis acid/base functionalized dibenzo[a,j]anthracene.

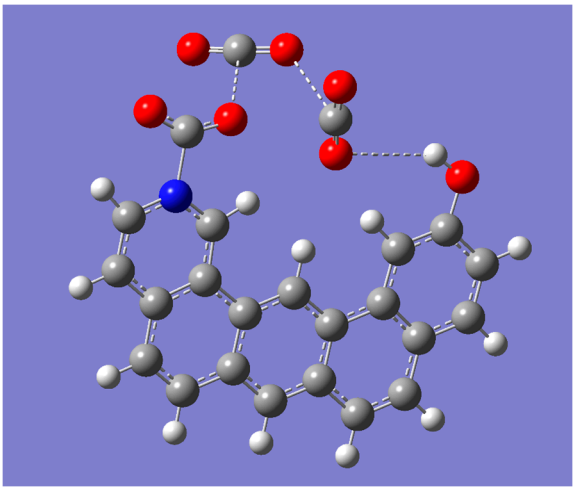

Figure 9. Optimized energy minimum structure for the interaction of the model Lewis acid/base functionalized dibenzo[a,j]anthracene (Figure 8) with CO_2. Selected bond lengths and angles: N ··· C = 1.633 Å, H ··· O = 2.994 Å, C ··· O = 2.545 and 2.729 Å, O–C–O = 140.1°, 175.3° and 173.8°.

3. Experimental Section

3.1. Computational Methods

Ab initio all electron molecular orbital (MO) calculations utilized non-local, gradient corrected density functional theory were performed using the Gaussian09 suite of programs [28]. For these molecules, relativistic effects were trivial and hence not taken into account. Optimization of all structures was carried out at the Hartree-Fock level with the 3-21G(*) basis set [29,30]. We have previously shown this basis set to give acceptable predictions of structural parameters for main group compounds [20,31–33]. To determine the relative energy of each species with electron correlation included, second order Møller-Plesset (MP2) calculations were performed [29].

3.2. Synthesis and Characterization of N- and S-Doped Porous Carbons

Sulfur and nitrogen containing porous carbon samples (SPC and NPC, respectively) were synthesized according to the protocol described previously [1,7]. Additional NPC samples were prepared using sodium metaborate tetrahydrate ($NaBO_2.4H_2O$, Sigma Aldrich, St. Louis, MO, USA) or borax ($Na_2B_4O_7$, Sigma Aldrich) as the activating agent. In a typical preparation, 300 mg of polyacrylonitrile (PAN, average molecular weight 150,000, Sigma Aldrich) and 300 mg of sodium metaborate tetrahydrate were mixed in a mortar and the mixture was activated by heating at 600 °C under Ar flow (600 sccm) for 1 h. For activation by borax, 400 mg of PAN was mixed with 800 mg of borax and activated under similar condition. Finally, activated material was washed with 1 L distilled water and dried in an oven at 80 °C for 12 h.

Samples were characterized by X-ray photoelectron spectroscopy. Measurements carried out in a PHI Quantera scanning XPS microprobe (Physical Electronics, Chanhassen, USA). The wt % of chemical elements was determined by XPS survey scans with pass energy of 140 eV. For detailed elemental analysis high resolution multi-cycle elemental scans with pass energy 26 eV was performed. Each spectrum was then deconvoluted by appropriate basis functions. Before spectral fitting, each spectrum was corrected for reference binding energy for C1s to 284.8 eV. The volumetric uptake measurements (sorption and desorption) of CO_2 and CH_4 were performed in an automated Sievert instrument (Setaram PCTPRO, Caluire, France) [34]. Various PC samples were first crushed into powders and packed in a stainless steel autoclave sample cell. Initial sample pretreatment was carried out at 130 °C for 1.5 h under high vacuum. The free volume inside the sample cell was determined by

a series of calibration procedures done under helium. Gas uptake experiments were carried out with high purity research grade CO_2 (99.99% purity, Matheson TRIGAS, Basking Ridge, NJ, USA).

4. Conclusions

In summary, we have shown that the reported formation of poly-CO_2 is unlikely to involve just the N or S substituents in NPC and SPC, respectively. Instead, if poly-CO_2 is formed it most likely is due to the presence of a Lewis acid species in concert with a Lewis base species. The spectroscopic observation of poly-CO_2 [1] may have been due to other factors in the reported materials rather than simply the presence of S or N. This fits with the lack of such spectroscopic reports in prior samples prepared by identical synthetic routes [3,5–7]. Based upon our simplified model structures, known molecular derivatives [9,10], and the known association of Lewis acid sites with oxygen [25–27], we propose that the presence of oxygen in high activity porous carbon materials is equally (or more) important than heteroatoms such as N or S. This is the subject of our future experimental studies.

Acknowledgments: This work was supported by Apache Corporation, Inc., the Robert A. Welch Foundation (C-0002), and the Welsh Government Ser Cymru Programme.

Author Contributions: Andrew R. Barron performed the calculations and analyzed the data. Saunab Ghosh prepared the porous carbon samples and performed XPS analysis. Both authors created the Figures and contributed to the manuscript.

Conflicts of Interest: The authors declare no conflict of interest.

References

1. Hwang, C.-C.; Tour, J.J.; Kittrell, C.; Espinal, L.; Alemany, L.B.; Tour, J.M. Capturing carbon dioxide as a polymer from natural gas. *Nat. Commun.* **2014**, *5*, 3961. [CrossRef] [PubMed]
2. Hao, G.P.; Li, W.C.; Qian, D.; Lu, A.H. Rapid synthesis of nitrogen-doped porous carbon monolith for CO_2 capture. *Adv. Mater.* **2010**, *7*, 853–857. [CrossRef] [PubMed]
3. Sevilla, M.; Valle-Vigón, P.; Fuertes, A.B. N-doped polypyrrole-based porous carbons for CO_2 capture. *Adv. Funct. Mater.* **2011**, *14*, 2781–2787. [CrossRef]
4. Ello, A.S.; Yapo, J.A.; Trokourey, A. N-doped carbon aerogels for carbon dioxide (CO_2) capture. *Afr. J. Pure Appl. Chem.* **2013**, *7*, 61–66.
5. Chandra, V.; Yu, S.U.; Kim, S.H.; Yoon, Y.S.; Kim, D.Y.; Kwon, A.H.; Meyyappan, M.; Kim, K.S. Highly selective CO_2 capture on N-doped carbon produced by chemical activation of polypyrrole functionalized graphene sheets. *Chem. Commun.* **2012**, *48*, 735–737. [CrossRef] [PubMed]
6. Lillo-Rodenas, M.A.; Cazorla-Amoros, D.; Linares-Solano, A. Understanding chemical reactions between carbons and NaOH and KOH: An insight into the chemical activation mechanism. *Carbon* **2003**, *41*, 267–275. [CrossRef]
7. Sevilla, M.; Fuertes, A.B. Highly porous S-doped carbons. *Micropor. Mesopor. Mat.* **2012**, *158*, 318–323. [CrossRef]
8. Iota, V.; Yoo, C.S.; Cynn, H. Quartzlike carbon dioxide: An optically nonlinear extended solid at high pressures and temperatures. *Science* **1999**, *283*, 1510–1513. [CrossRef] [PubMed]
9. Carmona, E.; González, F.; Poveda, M.L.; Marin, J.M. Reaction of *cis*-$[Mo(N_2)_2(PMe_3)_4]$ with COP synthesis and characterization of products of disproportionation and the X-ray structure of a tetrametallic mixed-valence Mo^{II}–Mo^{V} carbonate with a novel mode of carbonate binding. *J. Am. Chem. Soc.* **1983**, *105*, 3365–3366.
10. Langer, J.; Imhof, W.; Fabra, M.J.; García-Orduna, P.; Görls, H.; Lahoz, F.J.; Oro, L.A.; Westerhausen, M. Reversible CO_2 fixation by iridium(I) complexes containing Me_2PhP as ligand. *Organometallics* **2010**, *29*, 1642–1651. [CrossRef]
11. Dreisbach, F.; Staudt, R.; Keller, J.U. High pressure adsorption data of methane, nitrogen, carbon dioxide and their binary and ternary mixtures on activated carbon. *Adsorption* **1999**, *5*, 215–227. [CrossRef]
12. Krooss, B.M.; van Bergen, F.; Gensterblum, Y.; Pagnier, H.J.M.; David, P. High-pressure methane and carbon dioxide adsorption on dry and moisture-equilibrated Pennsylvanian coals. *Int. J. Coal Geol.* **2002**, *51*, 69–92. [CrossRef]

13. Bae, J.-S.; Bhatia, S.K. High-pressure adsorption of methane and carbon dioxide on coal. *Energy Fuels* **2006**, *20*, 2599–2607. [CrossRef]
14. Himeno, S.; Komatsu, T.; Fujita, S. High-pressure adsorption equilibria of methane and carbon dioxide on several activated carbons. *J. Chem. Eng. Data* **2005**, *50*, 369–376. [CrossRef]
15. Mantina, M.; Chamberlin, A.C.; Valero, R.; Cramer, C.J.; Truhlar, D.G. Consistent van der Waals radii for the whole main group. *J. Phys. Chem.* **2009**, *113*, 5806–5812. [CrossRef] [PubMed]
16. Khattak, G.D.; Salim, M.A.; Wenger, L.E.; Gilani, A.H. X-ray photoelectron spectroscopy (XPS) and magnetization studies of iron-sodium borate glasses. *J. Non-Cryst. Solids* **1999**, *244*, 128–136. [CrossRef]
17. Branch, C.S.; van Poppel, L.G.; Bott, S.G.; Barron, A.R. Molecular structure of $(tBu)_3Al[O{=}C(OPh)_2]$. *J. Chem. Cryst.* **1999**, *29*, 993–996. [CrossRef]
18. Branch, C.S.; Bott, S.G.; Barron, A.R. Group 13 trihalide complexes of 9-fluorenone: A comparison of methods for assigning relative Lewis acidity. *J. Organomet. Chem.* **2003**, *666*, 23–34. [CrossRef]
19. Power, M.B.; Bott, S.G.; Clark, D.L.; Atwood, J.L.; Barron, A.R. The interaction of organic carbonyls with sterically crowded aryloxide compounds of aluminum. *Organometallics* **1990**, *9*, 3086–3097. [CrossRef]
20. Francis, J.A.; McMahon, C.N.; Bott, S.G.; Barron, A.R. Steric effects in aluminum compounds containing monoanionic potentially bidentate ligands: Towards a quantitative measure of steric bulk. *Organometallics* **1999**, *18*, 4399–4416. [CrossRef]
21. Taylor, R.; Kennard, O. Hydrogen-bond geometry in organic crystals. *Acc. Chem. Res.* **1984**, *17*, 320–326. [CrossRef]
22. Vogelson, C.T.; Edwards, C.L.; Kobylivker, A.N.; Chacko, S.B.; Moran, C.E.; Dalton, K.; Stewart, S.M.; Werner, B.C.; Bott, S.G.; Barron, A.R. Molecular structure of $M(tfac)_3$ (M = Al, Co) and $Cu(H_2O)(fod)_2$: Examples of unusual supramolecular architecture. *J. Chem. Cryst.* **1998**, *28*, 817–824. [CrossRef]
23. Bishop, M.; Bott, S.G.; Barron, A.R. Structural characterization of borate esters in which sodium acts as a support to the structural framework. *J. Chem. Soc. Dalton Trans.* **2000**, *18*, 3100–3105. [CrossRef]
24. Goddard, R.; Niemeyer, C.M.; Reetz, M.T. Structure of 1,3-xylyl-(18-crown-5)-ammonium catecholborate (1/1). *Acta Cryst.* **1993**, *49*, 402–404. [CrossRef]
25. Lopez-Ramon, M.V.; Stoeckli, F.; Moreno-Castilla, C.; Carrasco-Marin, F. On the characterization of acidic and basic surface sites on carbons by various techniques. *Carbon* **1999**, *37*, 1215–1221. [CrossRef]
26. Barton, S.S.; Evans, M.J.B.; Halliop, E.; MacDonald, J.A.F. Acidic and basic sites on the surface of porous carbon. *Carbon* **1997**, *35*, 1361–1366. [CrossRef]
27. Boehm, H.P. Surface oxides on carbon and their analysis: A critical assessment. *Carbon* **2002**, *40*, 145–149. [CrossRef]
28. Frisch, M.J.; Trucks, G.W.; Schlegel, H.B.; Scuseria, G.E.; Robb, M.A.; Cheeseman, J.R.; Scalmani, G.; Barone, V.; Mennucci, B.; Petersson, G.A.; *et al*. *Gaussian 09*; Revision B.01; Gaussian Inc.: Wallingford, CT, USA, 2009.
29. Møller, C.; Plesset, M.S. Note on an approximation treatment for many-electron systems. *Phys. Rev.* **1934**, *46*, 618–622. [CrossRef]
30. Binkley, J.S.; Pople, J.A. Møller–Plesset theory for atomic ground state energies. *Int. J. Quantum Chem.* **1975**, *9*, 229–236. [CrossRef]
31. Ogrin, D.; Bott, S.G.; Barron, A.R. Molecular structure of $[Me_2Al(\mu\text{-}OPh)]_2$: A crystallographic and *ab initio* study. *J. Chem. Cryst.* **2008**, *38*, 397–401. [CrossRef]
32. Keys, A.; Brain, P.T.; Morrison, C.A.; Callender, R.L.; Smart, B.A.; Wann, D.A.; Robinson, H.E.; Rankin, D.W.H.; Barron, A.R. Molecular structures of $M(Bu^t)_3$ (M = Al, Ga, In) using gas-phase electron diffraction and *ab initio* calculations: Experimental and computational evidence for charge-transfer processes leading to photodissociation. *Dalton Trans.* **2008**, *3*, 404–410. [CrossRef] [PubMed]
33. Barron, A.R. What is the reason for the anomalous C-substituent effects in the Lewis acid catalyzed thermal decomposition of $[Me_2Al(\mu\text{-}OR)]_2$? *Main Group Chem.* **2015**, *14*, 87–96. [CrossRef]
34. Andreoli, E.; Dillon, E.P.; Cullum, L.; Alemany, L.B.; Barron, A.R. Cross-linking amine-rich compounds into high performing selective CO_2 absorbents. *Sci. Rep.* **2014**, *4*, 7304. [CrossRef] [PubMed]